Pergamon

Mech. Mach. Theory Vol. 32, No. 3, pp. 375–389, 1997

PII: S0094-114X(96)00033-X
0094-114X/97 $17.00 + 0.00

SINGULARITY ANALYSIS OF PLATFORM-TYPE MULTI-LOOP SPATIAL MECHANISMS

DHEEMAN BASU and ASHITAVA GHOSAL
Department of Mechanical Engineering, Indian Institute of Science, Bangalore-560 012, India

(Received 6 February 1995; in revised form 1 April 1996)

Abstract—In parallel manipulators and multi-loop mechanisms, singularity is associated with either loss or gain of a degree of freedom. This paper deals with the singularity analysis associated with gain of degree of freedom in a class of spatial mechanisms. We present a geometric condition for platform-type, multi-loop, mechanisms and parallel manipulators, containing spherical joints on the platform, whose existence ensures singularity in such mechanisms. The geometric condition is based on the concept of a common tangent. We show that this condition also implies that the determinant of certain matrices, formed by the differentiation of the loop-closure equations, are zero. We illustrate our results with the help of several multi-loop mechanisms. In particular, we describe the singularity surface for the three-degree-of- freedom RPSSPR–SPR 'wrist' mechanism.

1. INTRODUCTION

The singularities and workspace of serial manipulators have been studied extensively by several researchers and are very well understood. The singularities in serial manipulators are characterised by the loss of one or more degrees of freedom. At singular configurations, there exists a geometric condition that all joint axes intersect a line (called the 'extreme distance line' [1]) and the determinant of the manipulator Jacobian becomes zero. Singularities have been explained, in the most general form, by the use of screw theory [2, 3]. In the case of parallel manipulators and multi-loop mechanisms, singularity analysis is much more difficult due to increased complexity —multi-loop mechanisms can contain multi-degree-of-freedom joints (such as cylindric (C) or spherical (S)) and some of the joints may not be actuated. It has been shown that singularity, in multi-loop mechanisms, is associated with either a loss or a gain of a degree of freedom [4]. It is, however, very difficult to develop algebraic or geometric conditions for singularities in parallel manipulators and multi-loop mechanisms. In this paper, we present a geometric condition for a class of multi-loop, platform-type, mechanisms containing one or more loops with an S—S link†. This paper is organised as follows: In the rest of this section, we present a survey of the relevant literature. In Section 2, we present the concept of a loop-closure equation, define the concept of singularity and the associated concept of mobility in spatial mechanisms. In Section 3, we present our geometric condition and show that it is equivalent to the algebraic conditions of Section 2. In Section 4, we illustrate our results with a three-degree-of-freedom RPSSPR-SPR 'wrist' mechanism. Finally, in Section 5, we present our conclusions.

1.1. Literature survey

The mobility charts for single-loop, single-degree-of-freedom mechanisms were first developed by Radcliffe and Gupta [5]. Angeles and Callejas [6] and, later, Angeles and Bernier [7] and Williams and Reinholtz [8] considered the problem of four-bar linkages and used the concept of linkage discriminant. Rastegar [9, 10] has developed Grashof-type movability criteria for a number of single-loop, single-degree-of-freedom mechanisms by considering the mechanism to be a coupling of two serial chains. Ting [11] approached the problem geometrically and provided a simple movability criterion for a general N-bar linkage.

†In this paper, we will use the phrase 'S—S link' to denote the part of the loop (or the mechanism) containing two adjacent spherical joints.

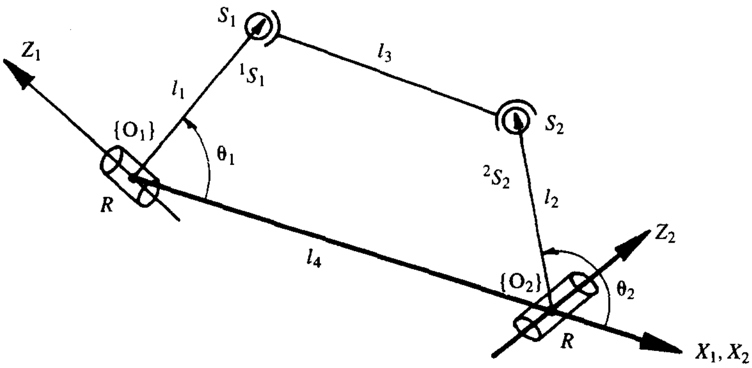

Fig. 1. The RSSR mechanism.

Litvin *et al.* [12] introduced a scheme of differentiating the product of all the consecutive transformation matrices in a loop, thereby obtaining six simultaneous equations defining a singularity configuration. The loop was restricted to consist of prismatic, revolute and cylindrical joints. Later, Fanghella [13] systematized a structure-based approach for the kinematic analysis of spatial linkages based on the algebra of groups. Gosselin and Angeles [4] assumed the number of outputs to be equal to the number of inputs and introduced the concept of two Jacobian matrices for parallel manipulators. The singularity of each matrix corresponds to loss or gain of degree of freedom and singularity of both occurs only when the mechanism is architecturally singular. Merlet [14] has obtained singular configurations of parallel manipulators using Grassman geometry. Recently, Hunt *et al.* [15] established the general kinematic principles of fully in-parallel and fully in-series devices. Through screw theory, they have shown that a workpiece grasped by a fully in-series manipulator can only lose freedom while a workpiece grasped by a fully in-parallel manipulator can only gain freedom. A hybrid manipulator may both lose and gain freedom.

2. LOOP-CLOSURE EQUATION AND SINGULARITY

The degree of freedom of any spatial mechanism is given by the well-known Grübler formula

$$f = 6(n - j - 1) + \sum_{i=1}^{j} f_i \tag{1}$$

where n is the number of links, j is the number of joints and f_i is the degree of freedom of the ith joint. The number of actuated joints is equal to f and is smaller than the total number of joints j in the mechanism. In order to obtain the values of the $(j - f)$ passive joints, one has to use the loop-closure constraint equations. To arrive at the 'simplest' form of the loop-closure equation one has to use the geometry of the mechanism and the nature of the joint. We illustrate the method of obtaining the 'simplest' form of the loop-closure equation with the help of a familiar RSSR mechanism.

In an RSSR mechanism, as in Fig. 1, f is 2. If we neglect the rotational degree of freedom of the S—S link about itself, then the mechanism has one degree of freedom. We assign coordinate systems $\{O_1\}$, $\{O_2\}$ as shown in Fig. 1 and denote the coordinates of the centres of the two spherical joints by ${}^1\mathbf{S}_1$ and ${}^2\mathbf{S}_2$, respectively†. The position vectors ${}^1\mathbf{S}_1$ and ${}^2\mathbf{S}_2$ can be written by inspection as

$$\begin{aligned} {}^1\mathbf{S}_1 &= [l_1 \cos\theta_1 \quad l_1 \sin\theta_1 \quad 0 \quad 1]^T \\ {}^2\mathbf{S}_2 &= [l_2 \cos\theta_2 \quad l_2 \sin\theta_2 \quad 0 \quad 1]^T. \end{aligned} \tag{2}$$

The position vector of the centre of the spherical joint, S_1, can be written in the coordinate system $\{O_2\}$ as

$${}^2\mathbf{S}_1 = [R]\,{}^1\mathbf{S}_1 \tag{3}$$

where $[R]$ is a known 4×4 transformation matrix relating coordinate systems $\{O_1\}$ and $\{O_2\}$.

†The leading superscript denotes the coordinate system in which the position vector is described and the following subscript denotes the number of the spherical joint.

In order to obtain the expression for θ_2 in terms of the actuated joint θ_1, we make use of the geometrical fact that the length of the S—S link remains constant. The loop closure equation can be written as

$$({}^1\mathbf{S}_1 - {}^1\mathbf{S}_2) \cdot ({}^1\mathbf{S}_1 - {}^1\mathbf{S}_2) = l_3^2. \tag{4}$$

After some simplification, the loop-closure equation can be written as

$$(l_2 \cos\theta_2 - l_4)(r_{11}l_1 \cos\theta_1 + r_{12}l_1 \sin\theta_1) + l_2 \sin\theta_2(r_{21}l_1 \cos\theta_1 + r_{22}l_1 \sin\theta_1)$$
$$+ l_4 l_2 \cos\theta_2 - (1/2)(l_1^2 + l_2^2 + l_4^2 - l_3^2) = f(\theta_1, \theta_2) = 0 \tag{5}$$

where l_i, $i = 1, 2, 3, 4$, are the four link lengths and r_{ij} are the entries of $[R]$.

In case of multi-loop mechanisms containing S—S links, the number of independent loop-closure equations will be equal to the number of independent loops.

2.1. *Number of independent loops*

In this paper, the term independence of loop-closure equation is not used in the usual topological sense. Two loops will be considered independent if they give rise to two independent loop-closure equations. In multi-loop, platform-type mechanisms, the number of independent loops solely depends on the platform. It turns out that the number of independent loops is equal to the number of parameters required to define the geometric shape of the platform. A triangle is defined by three parameters, namely, the lengths of the three sides. Hence, the number of independent loop-closure equations for a mechanism with a triangular platform is three. For a quadrilateral platform, we have six independent loop-closure equations. For a hexagonal platform, such as a 6-6 Stewart platform, the number of loop-closure equations is 12.

It can also be seen that, for any spatial mechanism with m equivalent single-degree-of-fredom joints†, not counting the spherical joints, the number of loop-closure equations, l, is equal to $(m - f)$.

2.2. *Singular configurations and mobility of a mechanism*

The loop-closure equation (5) can be used to solve for θ_2 for given values of θ_1. Depending on the link lengths and the r_{ij}s, we can obtain real or imaginary values of θ_2 for a given θ_1. If θ_2 is imaginary, then the mechanism cannot be assembled in that configuration. Likewise, for a given θ_2, θ_1 can also be real or imaginary. The range of real values of θ_1 and θ_2 determines the mobility of the mechanism. The extreme values of these ranges are the singular configurations of the mechanism.

The extreme singular configurations can also be obtained by differentiating the loop-closure relations. For the RSSR mechanism, we have

$$\frac{\partial f}{\partial \theta_1}\dot{\theta}_1 + \frac{\partial f}{\partial \theta_2}\dot{\theta}_2 = 0 \tag{6}$$

where $\dot{\theta}_i$ denotes the time derivative of θ_i.

At a singular configuration, $\dot{\theta}_1$ (or $\dot{\theta}_2$) is zero. For a non-trivial solution of the above equation (i.e. $\dot{\theta}_2$ (or $\dot{\theta}_1$) not equal to zero), the partial derivatives of f with respect to θ_2 (or θ_1) must be zero. Simultaneous solution of the loop-closure equation and the vanishing of the partial derivative of f gives the values of θ_1 and θ_2 where the mechanism is at a singular configuration. If we consider θ_1 to be the input, then for $\dot{\theta}_1$ equal to zero and $\dot{\theta}_2 \neq 0$, the mechanism is said to have gained a degree of freedom. On the other hand, if θ_2 is considered as the output, then for $\dot{\theta}_2$ equal to zero and $\dot{\theta}_1$ nonzero, the mechanism is said to have lost a degree of freedom. In this paper, we are interested only in the gain of one or more degrees of freedom.

In the case of the RSSR mechanism, the singular configurations and the mobility can be determined algebraically. However, for multi-loop and multi-degree-of-freedom mechanisms,

†A two-degree-of-freedom cylindrical (C) joint is equivalent to two one-degree-of-freedom joints.

algebraic expressions are often not possible to obtain and singular configurations need not be points (as in the case of RSSR mechanism) but can be curves, surfaces or higher-dimensional manifolds.

2.3. Multi-loop spatial mechanisms

Let us consider a general platform-type mechanism (containing S—S links on the platform) with m equivalent single-degree-of-freedom joints, not including the spherical joints and having f degrees of freedom. The l loop-closure equations can be written as

$$f_i(\theta_1, \theta_2, \ldots, \theta_m) = 0, \quad i = 1, 2, \ldots, l \tag{7}$$

where $\theta_1, \theta_2, \ldots, \theta_m$ are the m joint variables.

Differentiating the above loop-closure equations we can obtain l relations similar to equation (6). Without loss of generality we assume that first f of the m joints are actuated and the rest are passive. Hence, we can write the l velocity relations in a matrix form as

$$\begin{bmatrix} \frac{\partial f_1}{\partial \theta_1} & \frac{\partial f_1}{\partial \theta_2} & \cdots & \frac{\partial f_1}{\partial \theta_f} \\ \frac{\partial f_2}{\partial \theta_1} & \frac{\partial f_2}{\partial \theta_2} & \cdots & \frac{\partial f_2}{\partial \theta_f} \\ \vdots & \vdots & \ddots & \vdots \\ \frac{\partial f_l}{\partial \theta_1} & \frac{\partial f_l}{\partial \theta_2} & \cdots & \frac{\partial f_l}{\partial \theta_f} \end{bmatrix} \begin{bmatrix} \dot\theta_1 \\ \dot\theta_2 \\ \vdots \\ \dot\theta_f \end{bmatrix} + \begin{bmatrix} \frac{\partial f_1}{\partial \theta_{f+1}} & \frac{\partial f_1}{\partial \theta_{f+2}} & \cdots & \frac{\partial f_1}{\partial \theta_m} \\ \frac{\partial f_2}{\partial \theta_{f+1}} & \frac{\partial f_2}{\partial \theta_{f+2}} & \cdots & \frac{\partial f_2}{\partial \theta_m} \\ \vdots & \vdots & \ddots & \vdots \\ \frac{\partial f_l}{\partial \theta_{f+1}} & \frac{\partial f_l}{\partial \theta_{f+2}} & \cdots & \frac{\partial f_l}{\partial \theta_m} \end{bmatrix} \begin{bmatrix} \dot\theta_{f+1} \\ \dot\theta_{f+2} \\ \vdots \\ \dot\theta_m \end{bmatrix} = \begin{bmatrix} 0 \\ 0 \\ \vdots \\ 0 \end{bmatrix} \tag{8}$$

or

$$[J][\dot\theta] + [J^*][\dot\phi] = 0 \tag{9}$$

where $[\theta]$ is the vector of actuated joint variables or inputs $[\theta_1, \theta_2, \ldots, \theta_f]^{\mathrm{T}}$, and $[\phi] = [\theta_{f+1}, \theta_{f+2}, \ldots, \theta_m]^{\mathrm{T}}$ is the vector of passive joint variables. It may be noted that $[J^*]$ is always square, of dimension $l \times l$.

For the mechanism to gain a degree of freedom, we must have $[\dot\theta] = 0$ and $[\dot\phi] \neq 0$, which implies that

$$\det[J^*] = 0. \tag{10}$$

The above equation, when solved with the loop-closure equations, will give the singularity configurations of the mechanism.

In the case of the RSSR linkage, $l = 1$ and $[J^*]$ is 1×1. Assuming θ_1 to be the input, we can write the singularity condition as $\partial f/\partial\theta_2 = 0$. For the assumed coordinate system, $\partial f/\partial\theta_2 = 0$ expands to

$$\sin\theta_2(r_{11}l_3\cos\theta_1 + r_{12}l_3\sin\theta_1 + l_4) - \cos\theta_2(r_{21}l_2\cos\theta_1 + r_{22}l_2\sin\theta_1) = 0. \tag{11}$$

Solving equations (5) and (11), we can determine the points of singularity for an RSSR linkage.

In the case of one-degree-of-freedom mechanisms, the singularities are one-dimensional or points. In the case of f-degree-of-freedom mechanisms the singularities lie on an $(f-1)$-dimensional manifold. In degenerate cases, the singularities can also lie on lower-dimensional manifolds.

In the next section, we present a geometric condition and show that it is equivalent to the algebraic condition given in equation (10).

3. A GEOMETRIC APPROACH

Geometrically, a mechanism at a singularity configuration is always characterised by the existence of a common tangent at some joint. By this we mean that if the mechanism is cut at that joint and the two parts are allowed to move freely, keeping all the actuated joints of the mechanism locked, the loci of the two tips of the links will have a common tangent. This principle can be easily visualised with the help of a four-bar linkage. Figure 2(a) shows the linkage in a general non-singular configuration while Fig. 2(b) shows it in a singular configuration. If we cut the mechanism at joint j and allow rotation at the passive joints i and k only, keeping the input joint l locked, j_1 and j_2 (tips of links 1 and 2, respectively) describe circular arcs shown in Fig. 2. In

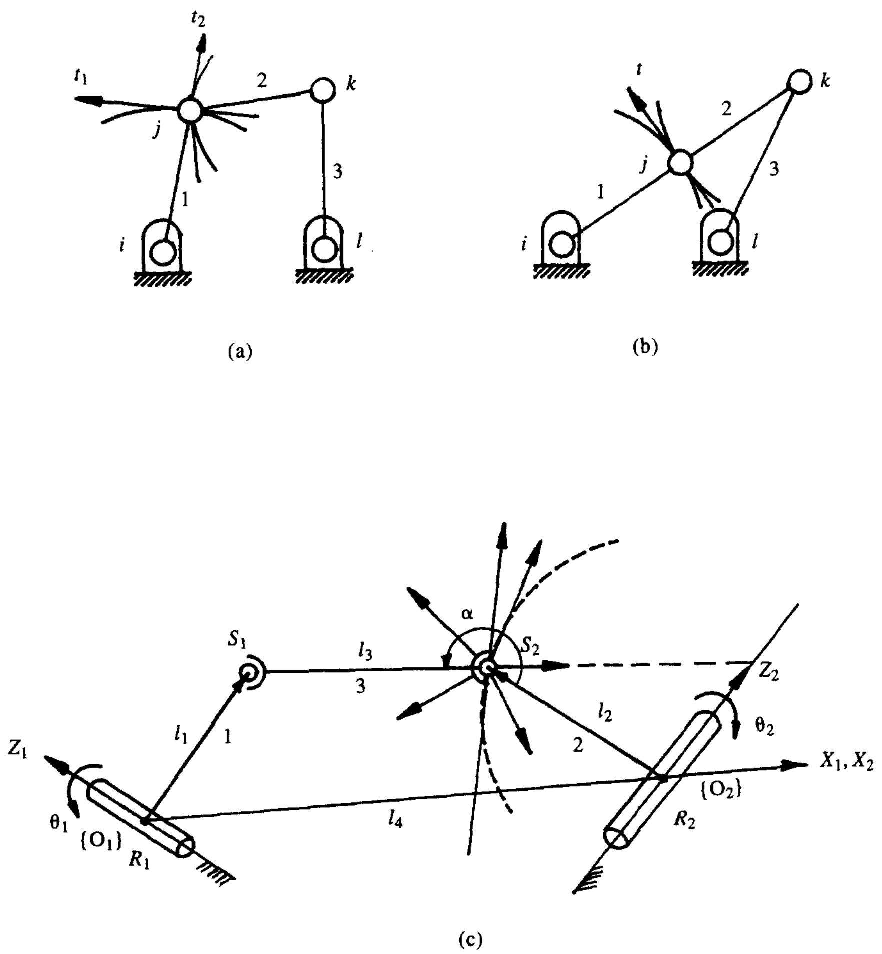

Fig. 2. Concept of a common tangent.

case 2(a), the tangents $\vec{t}_1$ and $\vec{t}_2$ are in different directions. In case 2(b), they are along a common direction $\vec{t}$.

The complexity of the above analysis increases with the number of degrees of freedom allowed at kinematic pairs and also with the number of loops. First, we develop the singularity criterion for the RSSR single-loop mechanism, and then extend the criterion to multi-loop mechanisms such as the RSSR–SC and RSSRR–SRR mechanisms.

Consider the RSSR mechanism shown in Fig. 2(c). We assume that the revolute joint R_1 is the actuated joint. If R_1 is locked, the centre of S_1 is fixed and singularity is possible only due to joint S_2. Breaking the joint S_2 and allowing the links to move freely with the actuated joint R_1 locked, we find that

(1) The locus of S_{21}, the tip of link 2, is a circle in a plane perpendicular to the joint axis $\vec{Z}_2$ and perpendicular to the line $\overline{O_2S_2}$.†

(2) The locus of S_{23}, the tip of link 3, is a spherical surface with centre at joint S_1 and with radius equal to l_3.

At a singular configuration, the common tangent $\vec{t}$ must be perpendicular to lines $\overline{O_2S_2}$, $\overline{S_1S_2}$ and to the axis $\vec{Z}_2$. Since the lines $\overline{O_2S_2}$ and $\overline{S_1S_2}$ intersect, we conclude that at a singular configuration, the lines $\overline{O_2S_2}$, $\overline{S_1S_2}$ and the joint axis $\vec{Z}_2$ lie on the same plane. Let us denote the angle from the

†The point O_i is the origin of the coordinate system $\{O_i\}$ and $\overline{O_iS_i}$ is the line joining the point O_i and the centre of the spherical joint S_i. Likewise the line $\overline{S_iS_j}$ is the line connecting the centres of the spherical joints S_i and S_j.

line $\overline{O_2S_2}$ to the line $\overline{S_1S_2}$ by α as shown in Fig. 2(c). The position vectors of the spherical joint S_1 in coordinate system $\{O_2\}$ can be written as

$$ {}^2\mathbf{S}_1 = [(l_2 - l_3 \cos\alpha)\cos\theta_2 \quad (l_2 - l_3\cos\alpha)\sin\theta_2 \quad -l_3\sin\alpha \quad 1]^T. \tag{12} $$

Using equations (3) and (12), we obtain

$$ (l_2 - l_3\cos\alpha)\cos\theta_2 = r_{11}l_1\cos\theta_1 + r_{12}l_1\sin\theta_1 + l_4 \tag{13} $$

$$ (l_2 - l_3\cos\alpha)\sin\theta_2 = r_{21}l_1\cos\theta_1 + r_{22}l_1\sin\theta_1 \tag{14} $$

$$ -l_3\sin\alpha = r_{31}l_1\cos\theta_1 + r_{32}l_1\sin\theta_1\,. \tag{15} $$

Eliminating $(l_2 - l_3\cos\alpha)$ from equations (13) and (14), we obtain the singularity condition of equation (11). In addition, after some algebra, we can obtain the loop-closure equation (5). This proves that the above equation set is equivalent to equations (5) and (11), which were obtained by an algebraic approach and the geometric condition is equivalent to $\partial f/\partial\theta_2 = 0$. We can thus conclude that: in a loop containing an S—S link, if the line joining the centres of the spherical joints intersects any passive R joint axis, the loop becomes singular. Also, the partial derivative of the loop-closure function with respect to that particular R joint variable becomes zero.

In the case of multi-loop mechanisms, singularity in one loop causes singularity of the mechanism, though the converse is not necessarily true. This fact is illustrated in the next example.

3.1. Multi-loop mechanism

For the singularity analysis of multi-loop mechanisms, we consider two examples: (1) the one-degree-of-freedom RSSR–SC mechanism shown in Fig. 3 and (2) the two-degree-of-freedom RSSRR–SRR mechanism shown in Fig. 4.

3.1.1. The RSSR–SC mechanism. Figure 3 shows the RSSR–SC mechanism with three coordinate systems, $\{O_1\}$, $\{O_2\}$ and $\{O_3\}$. Assuming that θ_1 is the actuated joint, when θ_1 is locked, the first link is fixed and singularity due to the spherical joint S_1 is impossible.

Next, we consider the possibility of singular configurations due to the spherical joint S_2. We cut the mechanism at S_2 and denote the point S_2 of the platform as S_{2p} and that of the link 2 as S_{2l}.

In the loop $R_1S_1S_3CR_1$, we have three joint variables which must satisfy the corresponding loop-closure equation. Hence, the degree of freedom of the loop is two. Out of these two freedoms, one is actuated and the other can be chosen arbitrarily. Hence, we get a planar pencil of tangents at S_{2p}. Since the centre of S_1 is fixed in space, the planar pencil must be perpendicular to the line $\overline{S_1S_2}$. In addition, the locus of S_{2l} is a circle and, therefore, the direction of the tangent to the locus is unique. At a singular configuration, a common tangent exists which must be perpendicular to the line $\overline{O_2S_2}$, the axis of the rotary joint R_2 and the line $\overline{S_1S_2}$. This is similar to the singularity in the one loop case discussed earlier.

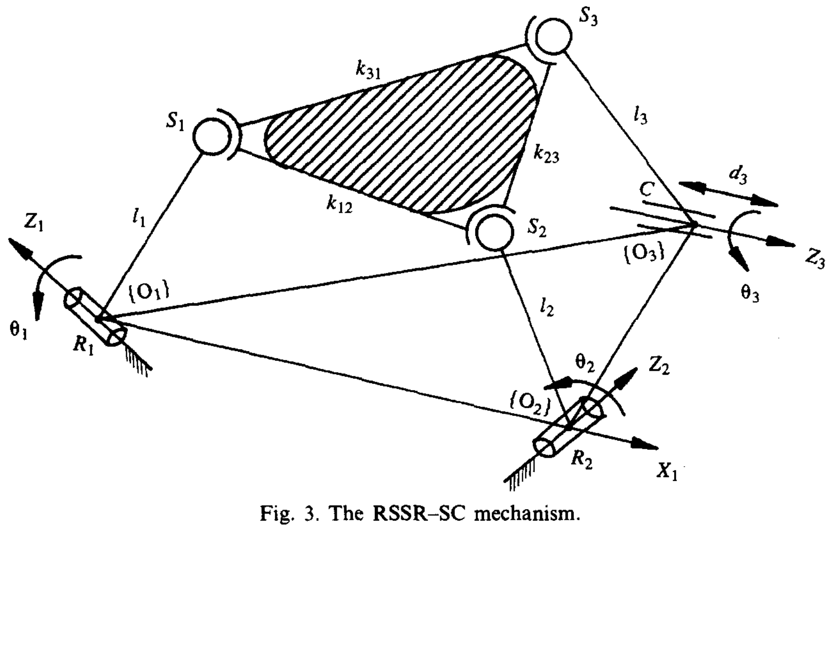

Fig. 3. The RSSR–SC mechanism.

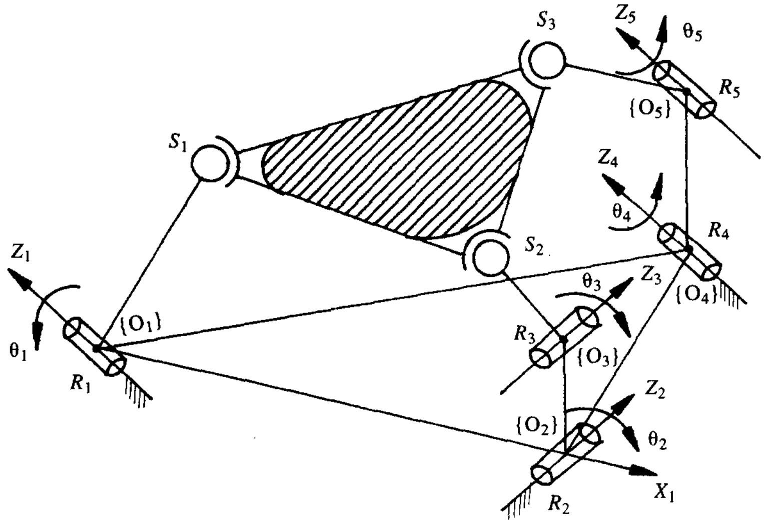

Fig. 4. The RSSRR–SRR mechanism.

Next we consider the possibility of singularity due to the spherical joint S_3. We cut the mechanism at joint S_3 and denote the point S_3 of the platform as S_{3p} and that of link 3 as S_{3l}. In the loop $R_1S_1S_2R_2R_1$, we have two joint variables which satisfy one loop-closure equation and one joint is actuated. Hence, the motion of the S_1—S_2 link is, in general, constrained and, for a locked input, the link S_1—S_2 is fixed in space. This implies a unique circular locus of S_{3p} and the tangent to this locus is perpendicular to the platform. The locus of S_{3l} is a cylindrical surface and, hence, we have a planar pencil of tangents at S_{3l}. This pencil is perpendicular to the line $\overline{O_3S_3}$ in link 3.

For the existence of common tangent, the line $\overline{O_3S_3}$ must be coplanar with the platform. To arrive at an algebraic expression for this type of singularity, we define three vectors $\vec{v}_1$, $\vec{v}_2$ and $\vec{v}_3$ along the lines $\overline{O_3S_3}$, $\overline{S_1S_3}$ and $\overline{S_2S_3}$, respectively. The three vectors are given by

$$\vec{v}_1 = \begin{bmatrix} s_{11}l_3\cos\theta_3 + s_{12}l_3\sin\theta_3 \\ s_{21}l_3\cos\theta_3 + s_{22}l_3\sin\theta_3 \\ s_{31}l_3\cos\theta_3 + s_{32}l_3\sin\theta_3 \end{bmatrix} \tag{16}$$

$$\vec{v}_2 = \begin{bmatrix} s_{11}l_3\cos\theta_3 + s_{12}l_3\sin\theta_3 + s_{13}d_3 - l_1\cos\theta_1 \\ s_{21}l_3\cos\theta_3 + s_{22}l_3\sin\theta_3 + s_{23}d_3 - l_1\sin\theta_1 \\ s_{31}l_3\cos\theta_3 + s_{32}l_3\sin\theta_3 + s_{33}d_3 \end{bmatrix} \tag{17}$$

$$\vec{v}_3 = \begin{bmatrix} s_{11}l_3\cos\theta_3 + s_{12}l_3\sin\theta_3 + s_{13}d_3 - r_{11}l_2\cos\theta_2 - r_{12}l_2\sin\theta_2 + l_{23x} \\ s_{21}l_3\cos\theta_3 + s_{22}l_3\sin\theta_3 + s_{23}d_3 - r_{21}l_2\cos\theta_2 - r_{22}l_2\sin\theta_2 + l_{23y} \\ s_{31}l_3\cos\theta_3 + s_{32}l_3\sin\theta_3 + s_{33}d_3 - r_{31}l_2\cos\theta_2 - r_{32}l_2\sin\theta_2 + l_{23z} \end{bmatrix} \tag{18}$$

where l_i, $i = 1, 2, 3$ are the link lengths and l_{23x}, l_{23y}, l_{23z}, r_{ij}, s_{ij} are the elements of the transformation matrices relating coordinate systems $\{O_2\}$ and $\{O_3\}$ to coordinate system $\{O_1\}$.

At a singular configuration, the triple product of these three vectors is zero, i.e.

$$v_1 \cdot (v_2 \times v_3) = 0. \tag{19}$$

We can also explain the above geometrical results as follows.

Along the lines of equation (4), we can obtain the following three loop-closure equations:

$$\begin{aligned} ({}^1\mathbf{S}_1 - {}^1\mathbf{S}_2)\cdot({}^1\mathbf{S}_1 - {}^1\mathbf{S}_2) &= k_{12}^2 \\ ({}^1\mathbf{S}_2 - {}^1\mathbf{S}_3)\cdot({}^1\mathbf{S}_2 - {}^1\mathbf{S}_3) &= k_{23}^2 \\ ({}^1\mathbf{S}_3 - {}^1\mathbf{S}_1)\cdot({}^1\mathbf{S}_3 - {}^1\mathbf{S}_1) &= k_{31}^2 \end{aligned} \tag{20}$$

where ${}^i\mathbf{S}_j$ is the position vector of the centre of the jth spherical joint in the ith coordinate system and the k_{ij}s are the lengths of the three sides of the platform. Differentiating the above equations, we obtain

$$\begin{bmatrix} C_{11} & C_{12} & 0 & 0 \\ 0 & C_{22} & C_{23} & C_{24} \\ C_{31} & 0 & C_{33} & C_{34} \end{bmatrix} \begin{bmatrix} \dot{\theta}_1 \\ \dot{\theta}_2 \\ \dot{\theta}_3 \\ \dot{d}_3 \end{bmatrix} = \begin{bmatrix} 0 \\ 0 \\ 0 \\ 0 \end{bmatrix} \tag{21}$$

where C_{ij} is the partial derivative of ith function with respect to the jth joint variable. With θ_1 as the input, at singularity, $\det[J^*] = 0$, and we can write

$$\det \begin{bmatrix} C_{12} & 0 & 0 \\ C_{22} & C_{23} & C_{24} \\ 0 & C_{33} & C_{34} \end{bmatrix} = 0. \tag{22}$$

The above equation can be written in the form

$$\det[A] \cdot \det[B] = 0$$

where $\det[A] = C_{12}$ and $\det[B] = C_{23}C_{34} - C_{24}C_{33}$. Therefore, at a singularity configuration, either $\det[A] = 0$ or $\det[B] = 0$. On simplification, $\det[A] = 0$ is found to be equivalent to singularity in the $R_1S_1S_2R_2R_1$ loop and $\det[B] = 0$ is equivalent to equation (19). It may be mentioned that $\det[B] = 0$ or the geometric condition equation (19) does not correspond to any single loop becoming singular.

3.1.2. The RSSRR–SRR mechanism. To develop the geometric concept further, we next consider a two-degree-of-freedom RSSRR–SRR mechanism. Figure 4 shows the RSSRR–SRR mechanism with coordinate systems, $\{O_1\}$, $\{O_2\}$ and $\{O_4\}$ attached to the three revolute joints at the base and coordinate systems $\{O_3\}$, $\{O_5\}$ attached to the revolute joints R_3 and R_5. For simplicity, we assume the axes of R_2 and R_3 are parallel. Similarly, the axes of R_4 and R_5 are assumed parallel. The RSSRR–SRR mechanism has two degrees of freedom, and we assume θ_1 and θ_2 to be the actuated joints. If the inputs are locked, the joint S_1 is fixed in space and cannot cause any singularity.

We next consider the possibility of singularity due to the spherical joint S_2. We cut the mechanism at joint S_2 and denote point S_2 of the platform as S_{2p} and that on link 2 as S_{2l}. In the loop $R_1S_1S_3R_5R_4R_1$, the number of degrees of freedom is two but only one joint is actuated. We can choose arbitrarily the rate of the R_1 joint and thus S_{2p} can move in a plane. Since S_1 is fixed, this plane is perpendicular to the line $\overline{S_1S_3}$. The locus of S_{2l} is a circle in a plane perpendicular to the joint axis of R_3 and, hence, has a unique tangent.

At a singular configuration, a common tangent exists which must be perpendicular to the line $\overline{S_2O_3}$, the axis of the rotary joint R_3 and also the line $\overline{S_1S_3}$. This is again the case of singularity in the first loop and, hence, is equivalent to the vanishing of the partial derivative of the first loop-closure function, with respect to θ_3. Since the loop has two degrees of freedom, we expect the singularities to occur along a curve.

Finally, we consider the possibility of singularity due to the spherical joint S_3. We cut the mechanism at joint S_3 and denote the point S_3 of the platform and of the link as S_{3p} and S_{3l}, respectively. In the loop $R_1S_1S_2R_3R_2R_1$, we have two degrees of freedom and two actuated joints. Therefore, the motion of the link S_1–S_2, in general, is constrained. The locus of S_{3p} is a circle with unique direction of the tangent. The direction of the tangent is necessarily perpendicular to the plane of the platform. The locus of S_{3l} is in a plane perpendicular to the axis of the joint R_5 because we have two passive joints in this leg. However, the tangent will lie in this plane and is, therefore, perpendicular to the axes of the joints R_4 and R_5.

If a common tangent exists, it has to be perpendicular to the plane of the platform as well as to the axis of the joint R_5. Thus, in the possible singular configuration, link 5 is aligned with the platform. This introduces two independent conditions, namely, the lines $\overline{S_1S_3}$ and $\overline{S_2S_3}$ intersect the axis of R_5. Equivalently, we can say that the partial derivatives of both second and third loop-closure functions with respect to θ_4 are zero. Hence, in this case we do not obtain any singularity curve and the singularity curve degenerates into a finite set of points.

We can also explain the above geometrical results as follows.

Along the lines of equation (4) we obtain three loop-closure equations similar to equation (20). Differentiating the loop-closure equations we obtain

$$\begin{bmatrix} C_{11} & C_{12} & C_{13} & 0 & 0 \\ 0 & C_{22} & C_{23} & C_{24} & C_{25} \\ C_{31} & 0 & C_{33} & C_{34} & C_{35} \end{bmatrix} \begin{bmatrix} \dot\theta_1 \\ \dot\theta_2 \\ \dot\theta_3 \\ \dot\theta_4 \\ \dot\theta_5 \end{bmatrix} = \begin{bmatrix} 0 \\ 0 \\ 0 \\ 0 \\ 0 \end{bmatrix} \tag{23}$$

where C_{ij} is the partial derivative of ith function with respect to jth joint variable. With θ_1 and θ_2 as inputs, at the singularity, $\det[J^*] = 0$, i.e.

$$\det \begin{bmatrix} C_{13} & 0 & 0 \\ C_{23} & C_{24} & C_{25} \\ 0 & C_{34} & C_{35} \end{bmatrix} = 0. \tag{24}$$

The above equation can be written in the form

$$\det[A] \cdot \det[B] = 0$$

where $\det[A] = C_{13}$ and $\det[B] = C_{24}C_{35} - C_{25}C_{34}$. We can see that $\det[A] = 0$ gives the condition of singularity due to the spherical joint S_2. The expression, $\det[B] = 0$, should give another singularity curve, but by means of geometric reasoning it can be shown that $\det[B] = 0$ does not correspond to any singularity curve. The expression, $\det[B] = 0$, degenerates to a finite set of points where $C_{24} = C_{34} = 0$. This fact was verified numerically.

3.2. *Summary*

The concept of a common tangent is a useful tool to visualise the singular configurations of platform-type spatial mechanisms containing S—S links. The results obtained from the use of this concept are in complete agreement with the algebraic results obtained from differentiating loop-closure equations. The main results are:

(1) In a loop containing an S—S link, if the line joining the centres of the adjacent S joints intersects any passive R joint, the mechanism is in a singular configuration.

(2) In the above situation, the partial derivative of the loop-closure function with respect to the rotation at the R joint is zero.

(3) In multi-loop mechanisms, in addition to the singular configurations, resulting from condition (1), there are other singularities where condition (1) may not be true. In such situations other geometrical conditions are needed.

4. SINGULARITY OF RPSSPR-SPR MECHANISM

In Ref. [16], the three-loop, three-degree-of-freedom RPSSPR–SPR mechanism of Fig. 5 has been proposed as a parallel 'wrist'. The authors have given the inverse and direct kinematics of this mechanism, however, they have not described its singularities. It is important to know the singularities of this mechanism before it can be used. In this section, we obtain the singularities of this mechanism by making use of the approach described in Sections 2 and 3.

4.1. *Algebraic and geometric approach*

We choose the geometry and the coordinate systems used in Ref. [16]. The chosen geometry causes loss of generality to some extent but makes the expressions much simpler. The revolute joint axes are assumed to be coplanar and are perpendicular to the medians passing through the respective vertices of the equilateral base-triangle. In this mechanism all the spherical joints are

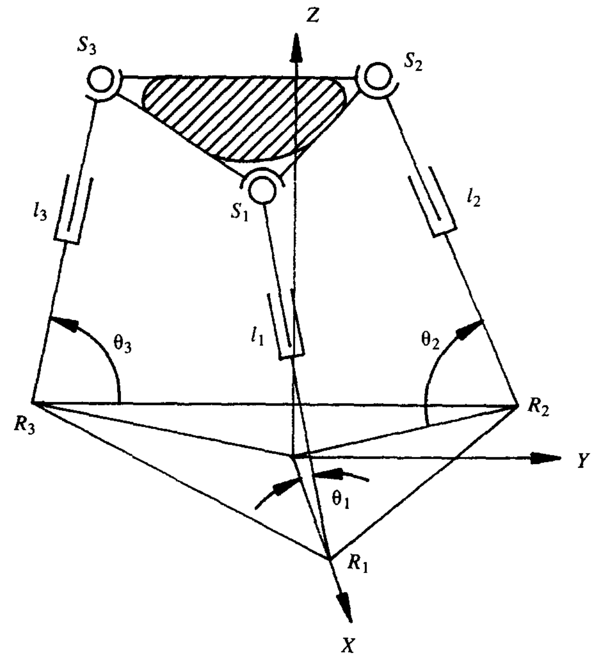

Fig. 5. The RPSSPR–SPR mechanism.

equivalent, since the mechanism is symmetric. Therefore, it is enough to consider the possibility of singularity due to any particular spherical joint. We arbitrarily choose spherical joint S_1.

We denote the point S_1 on the platform and that on the first leg as S_{1p} and S_{1l} respectively. In the $R_2P_2S_2S_3P_3R_3$ loop, we have four degrees of freedom and only one loop-closure equation. Hence the loop has three degrees of freedom out of which two are actuated and one can be chosen arbitrarily. Therefore, the tangents at S_{1p} can lie in a solid region. Again, in the first leg we have two degrees of freedom and one of them, the prismatic one, is controlled. Hence we find that the locus of S_{1l} is a circle. The tangent in this case has a unique direction. The common tangent, if it exists, will lie on the vertical plane as well as on the planar pencil. By simple inspection, we can express the coordinates of the centres of the spherical joints as

$$^{1}\mathbf{S}_1 = [(1 - L_1\cos\theta_1) \quad 0 \quad L_1\sin\theta_1 \quad 1]^{\mathrm{T}}$$

$$^{1}\mathbf{S}_2 = \left[-\tfrac{1}{2}(1 - L_2\cos\theta_2) \quad \frac{\sqrt{3}}{2}(1 - L_2\cos\theta_2) \quad L_2\sin\theta_2 \quad 1\right]^{\mathrm{T}}$$

$$^{1}\mathbf{S}_3 = \left[-\tfrac{1}{2}(1 - L_3\cos\theta_3) \quad \frac{\sqrt{3}}{2}(1 - L_3\cos\theta_3) \quad L_3\sin\theta_3 \quad 1\right]^{\mathrm{T}}. \tag{25}$$

Since the lengths between the S joints are constant, we can write the three loop-closure equations as in equation (20). Differentiating the three loop-closure equations we obtain

$$\begin{bmatrix} A_{11} & A_{12} & 0 & D_{11} & D_{12} & 0 \\ 0 & B_{22} & B_{23} & 0 & E_{22} & E_{23} \\ C_{31} & 0 & C_{33} & F_{31} & 0 & F_{33} \end{bmatrix} \begin{bmatrix} \dot{L}_1 \\ \dot{L}_2 \\ \dot{L}_3 \\ \dot{\theta}_1 \\ \dot{\theta}_2 \\ \dot{\theta}_3 \end{bmatrix} = \begin{bmatrix} 0 \\ 0 \\ 0 \\ 0 \\ 0 \\ 0 \end{bmatrix}. \tag{26}$$

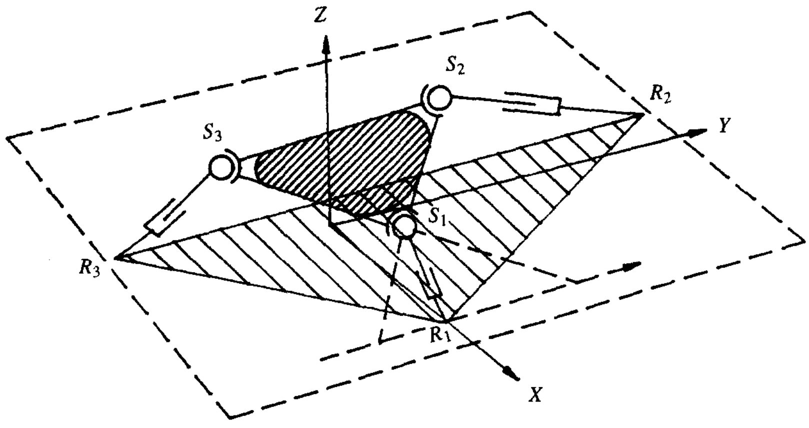

Fig. 6. Singularity corresponding to case 2 for S_1.

Let us consider variables L_i, associated with the prismatic joints, to be the inputs. The condition for the existence of singularities is

$$\det[J^*] = \det\begin{bmatrix} D_{11} & D_{12} & 0 \\ 0 & E_{22} & E_{23} \\ F_{31} & 0 & F_{33} \end{bmatrix} = 0$$

or

$$D_{11}E_{22}F_{33} + D_{12}E_{23}F_{31} = 0. \tag{27}$$

The above equation, together with the three loop-closure equations in six joint variables, defines the singularity surface. It is difficult to obtain explicitly an expression for this surface, since the singularity surface seems to be of a very high order. A number of particular cases can be, however, solved in closed form, which are the boundary curve or curves of symmetry of the singularity surface. We discuss these cases using the geometric and algebraic approaches described in this paper.

4.1.1. Case 1. Singularity may occur when one row of the Jacobian matrix, $[J^*]$, is zero. For example, let us consider $D_{11} = D_{12} = 0$. This means the line $\overline{S_1S_2}$ intersects the axes of the revolute joints R_1 and R_2. This can happen only when the line $\overline{S_1S_2}$ is on the plane of the base and, hence, both θ_1 and θ_2 are zero. Therefore, this case is not of much kinematic significance.

4.1.2. Case 2. Singularity may occur when any one column of the $[J^*]$ matrix is zero. For each column of the $[J^*]$ equated to zero, we obtain two equations (for example, the first column equated to zero yields $D_{11} = F_{31} = 0$). These equations, together with the three loop-closure equations, describe a curve. We can define a curve as the locus of the centroid of the platform. The curve corresponding to $D_{11} = F_{31} = 0$, with the length of the sides of the platform denoted by k, is given by

$$\begin{aligned} &-16k^2x^2z^2 + 64k^2x^3z^2 + 16x^4z^2 - 96k^2x^4z^2 - 64x^5z^2 + 64k^2x^5z^2 + 96x^6z^2 - 16k^2x^6z^2 \\ &- 64x^7z^2 + 16x^8z^2 - 24k^2x^2z^4 + 48k^2x^3z^4 + 32x^4z^4 - 24k^2x^4z^4 - 64x^5z^4 \\ &+ 32x^6z^4 + k^4z^6 - 8k^2x^2z^6 + 16x^4z^6 = 0. \end{aligned} \tag{28}$$

To give a geometric interpretation of this curve, we set joint rates of the passive rotary joints in the $R_2P_2S_2S_3P_3R_3$ loop to zero. Then, the line $\overline{S_2S_3}$ is fixed and the tangent at S_{1p} must be perpendicular to the platform. So, if a common tangent exists, the line $\overline{S_3S_1}$ and the line $\overline{S_2S_1}$ must intersect the joint R_1 axis. This is similar to Condition (1) described in the previous section, applied to the first and third loops. In this case, the mechanism gains one degree of freedom and this particular singularity occurs along three curves corresponding to the three legs. Figure 6 shows this singular configuration.

4.1.3. Case 3. Singularity may also occur when two terms of $[J^*]$, which are neither in the same row nor in the same column, are zero. This also results in three symmetrical curves. For $D_{12} = F_{36} = 0$, the equation of the curve is

$$\begin{aligned}
&-256k^2x^2 + 32k^4x^2 - k^6x^2 - 256k^2x^3 + 16k^4x^3 + 256x^4 - 128k^2x^4 + 3k^4x^4 + 256x^5 - 32k^2x^5 \\
&+ 96x^6 - 3k^2x^6 + 16x^7 + x^8 + 48k^2xz^2 - 12k^4xz^2 + 32x^2z^2 - 2k^2x^2z^2 - 6k^4x^2z^2 - 48x^3z^2 \\
&+ 2x^4z^2 + 4k^2x^4z^2 + 12x^5z^2 + 2x^6z^2 + z^4 - 2k^2z^4 + k^4z^4 - 4xz^4 + 4k^2xz^4 + 6x^2z^4 \\
&- 2k^2x^2z^4 - 4x^3z^4 + x^4z^4 = 0.
\end{aligned} \tag{29}$$

To give a geometric interpretation of this case, we consider the case of singularity due to more than one spherical joint. We consider common tangents at the spherical joints S_2 and S_3. Since the distance between S_2 and S_3 cannot change, the two common tangents must be parallel and the line $\overline{S_2S_3}$ moves in a plane. S_1 has to maintain a constant distance from S_2 and S_3 and from the axis of R_1. Hence, S_1 must be fixed in space. For this singular configuration, the line $\overline{S_1S_2}$ intersects the axis of R_2 and the line $\overline{S_1S_3}$ intersects the axis of R_3. This is equivalent to Condition (1) applied to two different loops and two different rotary joints. Mathematically, the partial derivatives of the first and third loop-closure functions with respect to θ_1 and θ_2, respectively, are equal to zero. This singularity also occurs along a curve, but the mechanism gains two degrees of freedom in this

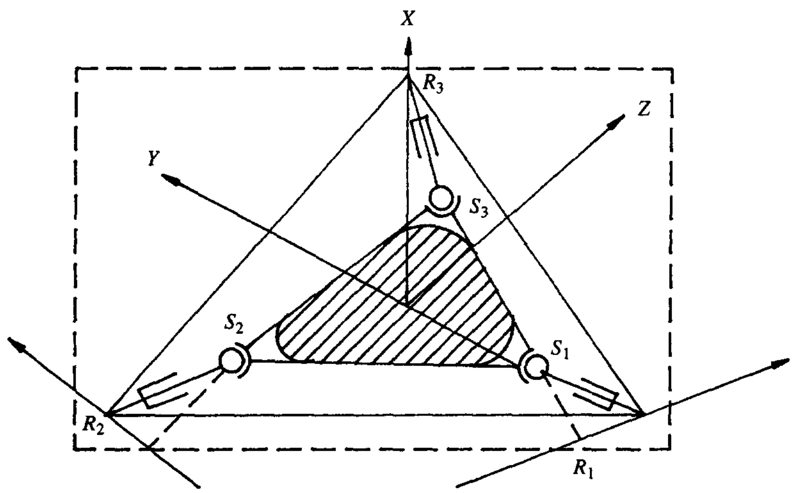

Fig. 7. Singularity corresponding to case 3 for S_2 and S_3.

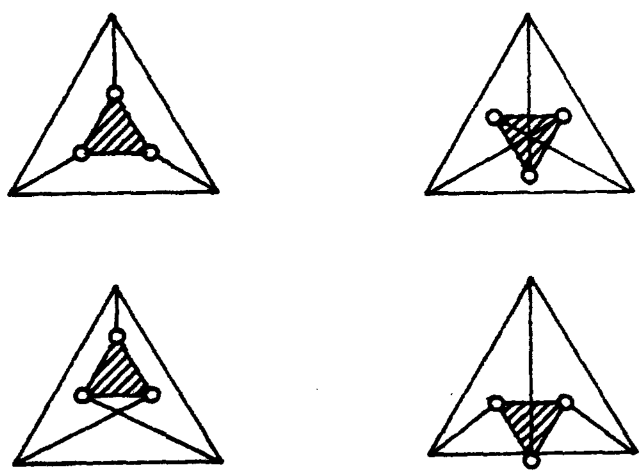

Fig. 8. Alignment of the platform with the base-special case.

case. This is the curve where the singularity surfaces of the spherical joints S_2 and S_3 intersect. Figure 7 shows the singular configuration.

4.1.4. A special case. Lastly, the singularity caused by all three spherical joints together is worth mentioning. In this case, the three common tangents are parallel to each other and all are perpendicular to the platform. Therefore, the platform is in the same plane as the base. In this case,

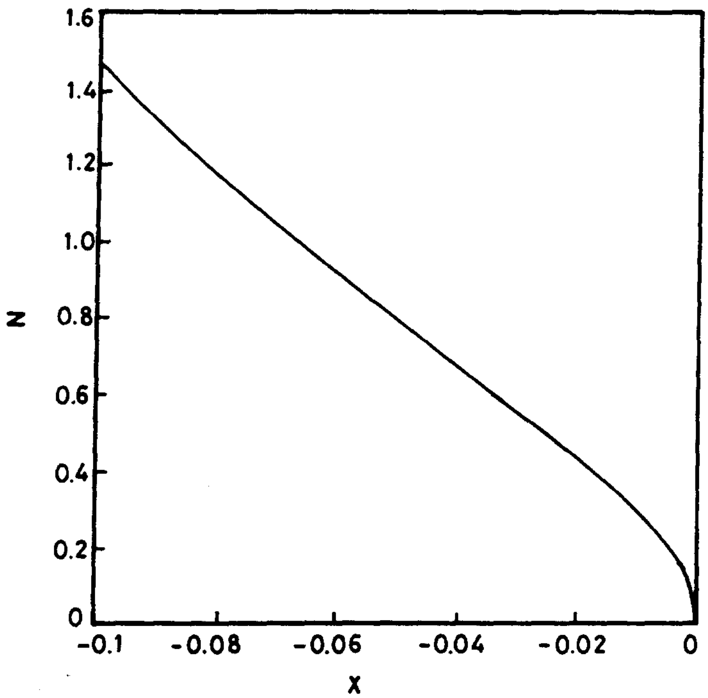

Fig. 9. Plot of singularity curve for case 2.

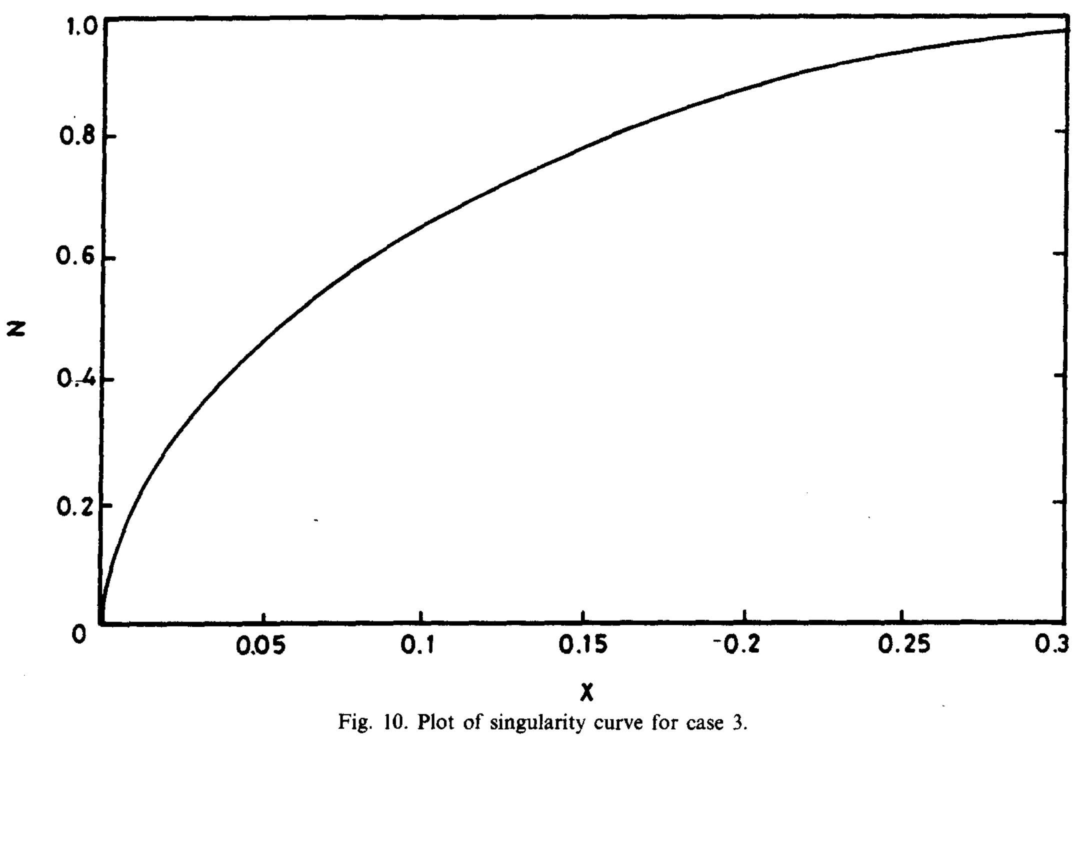

Fig. 10. Plot of singularity curve for case 3.

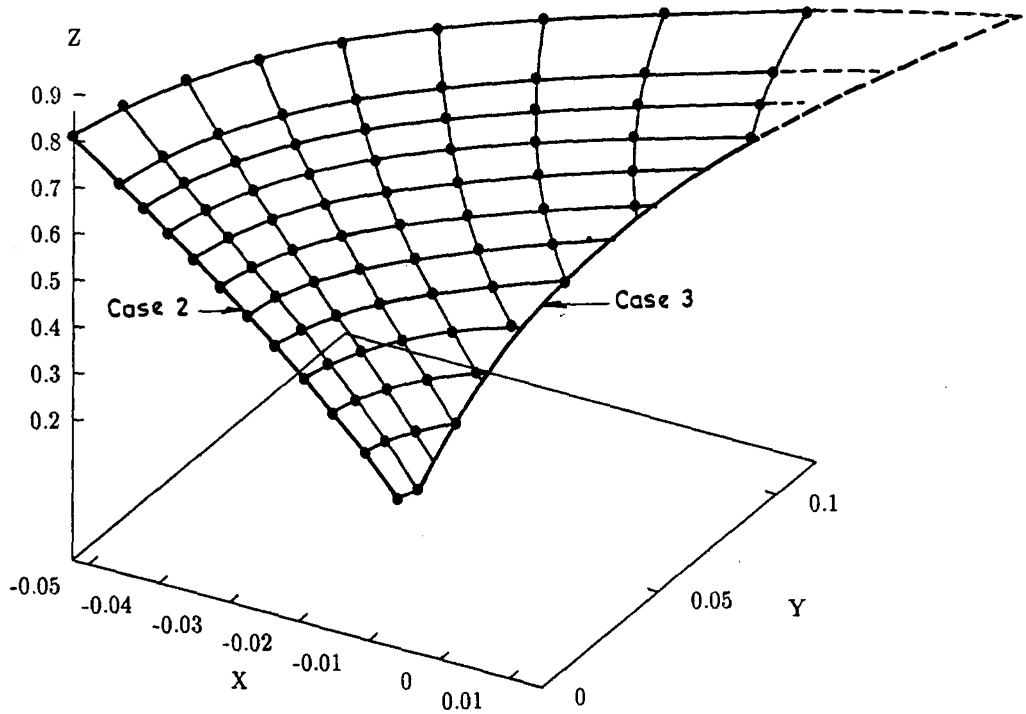

Fig. 11. Singularity surface for the RPSSPR–SPR mechanism.

the mechanism gains three degrees of freedom and this singularity can happen at a finite number of points. All the elements of the Jacobian matrix are zero in this case. Figure 8 shows the four possible ways the mechanism can be assembled with the platform in the same plane as the base.

4.2. *Numerical results*

For numerical results, the RPSSPR–SPR 'wrist' mechanism was assumed to have a base with unit sides and the platform with sides of 0.5 units. The ranges of all of the prismatic joints are assumed such that each leg can vary between 0.5–0.9 units. To obtain the singularity surface, we solve numerically equations (20) and (27). These are four equations in six variables, θ_1, θ_2, θ_3, L_1, L_2, L_3. It is difficult to solve these nonlinear equations numerically by brute force and the geometrical approach helped us obtain the initial guesses for the iterative solution method.

We plot the singularities as the locus of the centroid of the moving platform. Figure 9 shows a plot of the singularity curve corresponding to Case 2 and spherical joint S_1. Figure 10 shows the singularity curve for Case 3 and spherical joints S_2 and S_3. The singularity surface for the RPSSPR–SPR mechanism is shown in Fig. 11. From symmetry considerations, the mechanism has three identical singularity surfaces corresponding to the three spherical joints. Figure 11 shows only the singularity surface corresponding to S_1. Each surface is also symmetric about the singularity curve of Case 2 and we plot only one half of the singularity surface for better clarity. The other curve shown in Fig. 11 is the intersecting curve with the singularity surface of S_3. In Fig. 11, the numerically computed (X, Y, Z) coordinates are marked by the symbol •.

5. CONCLUSIONS

The singularities in multi-loop mechanisms associated with a gain of degree of freedom can be obtained by solving loop-closure equations together with the differential form of the loop-closure equation. It is, however, difficult to visualise the singularities from these equations. It is also difficult to arrive at the initial guesses required for numerical solution of these equations. In this paper, we have presented geometric conditions, based on the concept of a common tangent, which are useful in determining the singularities of multi-loop, platform type mechanisms containing spherical joints. The geometric conditions are equivalent to the conditions obtained from the differential form of the loop-closure equations and they help in giving a geometric interpretation of the algebraic results. The geometric conditions also help in determining the singularities numerically. The algebraic and geometrical approaches are used to determine the singularities of a parallel RPSSPR–SPR 'wrist' mechanism.

Acknowledgement—The authors wish to thank Bhaskar Dasgupta and the anonymous reviewers for their valuable comments.

REFERENCES

1. Sugimoto, K. and Duffy, J., *ASME Journal of Mechanical Design*, 1981, **103,** 631–636.
2. Hunt, K. H., *Kinematic Geometry of Mechanisms*. Clarendon Press, Oxford, 1978.
3. Sugimoto, K., Duffy J. and Hunt, K. H., *Mechanism and Machine Theory*, 1982, **17,** 119–132.
4. Gosselin, C. and Angeles, J., *IEEE Journal of Robotics and Automation*, 1990, **6**(3), 281–290.
5. Gupta, V. K. and Radcliffe, C. W., *Journal of Engineering for Industry, Transactions of ASME*, 1971, 125–130.
6. Angeles, J. and Callejas, M., *ASME Journal of Mechanisms, Transmissions and Automation in Design*, 1985, **106,** 327–332.
7. Angeles, J. and Bernier, A., *ASME Journal of Mechanisms, Transmissions and Automation in Design*, 1987, **109**(2), 197–203.
8. Williams, R. L. II and Reinholtz, C. F., *ASME Journal of Mechanisms Transmission and Automation Design*, 1987, **109,** 178–182.
9. Rastegar, J. and Tu, Q., *ASME Journal of Mechanical Design*, 1987, **109,** 178–182.
10. Rastegar, J., *Mechanism and Machine Theory*, 1992, **27**(5), 623–632.
11. Ting, K. L., *ASME Journal of Mechanisms, Transmission and Automation in Design*, 1989, **111,** 504–507.
12. Litvin, F. L., Fanghella, P., Tan, J. and Zhang, Y., *ASME Journal of Mechanisms, Transmission and Automation in Design*, 1986, **108,** 516–523.
13. Fanghella, P., *Mechanism and Machine Theory*, 1988, **23**(3), 171–183.
14. Merlet, J.-P., *International Journal of Robotics Research*, 1989, **8**(5), 45–56.
15. Hunt, K. H., Samuel, A. E. and McAree, P. R., *International Journal of Robotics Research*, 1991, **10**(2), 123–134.
16. Lee, K. M. and Shah, D., *IEEE Journal of Robotics and Automation*, 1988, **4**(3), 354–360.